

A Polarization Pursuers' Guide

Andrew H. Jaffe^{1*}, Marc Kamionkowski^{2,3†}, and Limin Wang^{2‡}

¹*Center for Particle Astrophysics, 301 LeConte Hall, University of California, Berkeley, CA 94720*

²*Department of Physics, 538 West 120th Street, Columbia University, New York, NY 10027*

³*California Institute of Technology, Mail Code 130-33, Pasadena, CA 91125*
(September 1999)

Abstract

We calculate the detectability of the polarization of the cosmic microwave background (CMB) as a function of the sky coverage, angular resolution, and instrumental sensitivity for a hypothetical experiment. We consider the gradient component of the polarization from density perturbations (scalar modes) and the curl component from gravitational waves (tensor modes). We show that the amplitude (and thus the detectability) of the polarization from density perturbations is roughly the same in any model as long as the model fits the big-bang-nucleosynthesis (BBN) baryon density and degree-scale anisotropy measurements. The degree-scale polarization is smaller (and accordingly more difficult to detect) if the baryon density is higher. In some cases, the signal-to-noise for polarization (both from scalar and tensor modes) may be improved in a fixed-time experiment with a smaller survey area.

I. INTRODUCTION

It has long been known that the cosmic microwave background (CMB) must be polarized if it has a cosmological origin [1,2]. Detection, and ultimately mapping, of the polarization will help isolate the peculiar velocity at the surface of last scatter [3], constrain the ionization history of the Universe [4], determine the nature of primordial perturbations [5,6], detect an inflationary gravitational-wave background [7,8], primordial magnetic fields [9–11], and

*jaffe@cfpa.berkeley.edu

†Email: kamion@tapir.caltech.edu

‡Email: limin@cuphyb.phys.columbia.edu

cosmological parity violation [12,13], and maybe more (see, e.g., Ref. [14] for a recent review). However, the precise amplitude and angular spectrum of the polarization depends on a structure-formation model and the values of numerous undetermined parameters. Moreover, it has so far eluded detection.

A variety of experiments are now poised to detect the polarization for the first time. But what is the ideal experiment? What angular resolution, instrumental sensitivity, and fraction of the sky should be targeted? Can it be picked out more easily by cross-correlating with the CMB temperature? The purpose of this paper is to answer these questions in a fairly model-independent way.

We first address the detectability of the gradient component of the polarization from density perturbations. *A priori*, one might expect the detectability of this signal to depend sensitively on details of the structure-formation model, ionization history, and on a variety of undetermined cosmological parameters. However, we find that if we fix the baryon-to-photon ratio to its big-bang-nucleosynthesis (BBN) value and demand that the degree-scale anisotropy agree with recent measurements, then the detectability of the polarization is roughly model-independent. We provide some analytic arguments in support of this result. We can thus specify an experiment that would be more-or-less guaranteed to detect the CMB polarization. Non-detection in such experiments would thus only be explained if the baryon density considerably exceeded the BBN value.

We then consider the curl component of the polarization from an inflationary gravitational-wave background. This extends slightly the work of Refs. [15,16].¹ The new twist here is that we consider maps with partial sky coverage (rather than only full-sky maps) and find that in a noise-limited fixed-time experiment, the sensitivity to gravitational waves may be improved considerably by surveying more deeply a smaller patch of sky.²

Since the polarization should be detected shortly, our main results on its detectability should, strictly speaking, become obsolete fairly quickly. Even so, our results should be of some lasting value as they provide figures of merit for comparing the relative value, in terms of signal-to-noise, of various future CMB polarization experiments. It should be kept in mind, however, that ours is a hypothetical experiment in which foregrounds have been subtracted and instrumental artifacts understood, and any comparison with realistic experiments must take these effects into account.

Section II briefly reviews the CMB polarization signals. Section III introduces the formalism for determining the detectability of polarization for a given experiment. Section IV considers polarization from scalar modes for a putative structure-formation model and Section V evaluates the detectability of the polarization from gravitational waves (using only the curl component of the polarization). Section VI presents the results of the prior two Sections in a slightly different way. Section VII shows that the results for scalar modes in Section IV would be essentially the same in virtually any other structure-formation model

¹There is also related work in Refs. [17–19] in which it is determined how accurately various cosmological and inflationary parameters can be determined in case of a positive detection.

²Similar arguments were investigated for temperature maps in Refs. [20,21].

with a BBN baryon density and degree-scale temperature anisotropy that matches recent measurements. We make some concluding remarks in Section VII.

II. BRIEF REVIEW OF CMB POLARIZATION

Ultimately, the primary goal of CMB polarization experiments will be to reconstruct the polarization power spectra and the temperature-polarization power spectrum. Just as a temperature (T) map can be expanded in terms of spherical harmonics, a polarization map can be expanded in terms of a set of tensor spherical harmonics for the gradient (G) component of the polarization and another set of harmonics for the curl (C) component [22,23]. Thus, the two-point statistics of the T/P map are specified completely by the six power spectra $C_\ell^{XX'}$ for $X, X' = \{T, G, C\}$. Parity invariance demands that $C_\ell^{TC} = C_\ell^{GC} = 0$ (unless the physics that gives rise to CMB fluctuations is parity breaking [12]). Therefore the statistics of the CMB temperature-polarization map are completely specified by the four sets of moments, C_ℓ^{TT} , C_ℓ^{TG} , C_ℓ^{GG} , and C_ℓ^{CC} . See, e.g., Fig. 1 in Ref. [15] for sample spectra from adiabatic perturbations and from gravitational waves.

There are essentially two things we would like to do with the CMB polarization: (1) map the G component to study primordial density perturbations, and (2) search for the C component due to inflationary gravitational waves [7,8]. The G signal from density perturbations is more-or-less guaranteed to be there at some level (to be quantified further below), and will undoubtedly provide a wealth of information on the origin of structure and the values of cosmological parameters. The amplitude of the C component from inflationary gravitational waves is proportional to the square of the (to-be-determined) energy scale of inflation. It is not guaranteed to be large enough to be detectable even if inflation did occur. On the other hand, if inflation had something to do with grand unification or Planck-scale physics, as many theorists surmise, then the polarization is conceivably detectable, as argued in Refs. [14,15,17] and further below. If detected, it would provide a unique and direct window to the Universe as it was 10^{-36} seconds after the big bang!

III. FORMALISM

We first address the general question of the detectability of a particular polarization component. We assume that the amplitude of the various polarization signals will each be picked out by a maximum-likelihood analysis [24]. The shape of the likelihood function will then give limits on the parameters, in this case the various power spectra, C_ℓ^{XX} that describe the CMB. In particular, the curvature of the likelihood gives traditional error bars, defined as for a Gaussian distribution (but see Ref. [25] for a discussion of the more complicated true non-Gaussian distribution). Here we will concentrate on the error bar for the overall amplitude of the power spectra.

We can then ask, what is the smallest amplitude that could be distinguished from the null hypothesis of no polarization component by an experiment that maps the polarization over some fraction of the sky with a given angular resolution and instrumental noise? This question was addressed (for the curl component) in Ref. [15] for a full-sky map. If an experiment concentrates on a smaller region of sky, then several things happen that affect

the sensitivity: (1) information from modes with $\ell \lesssim 180/\theta$ (where θ^2 is the area on the sky mapped) is lost;³ (2) the sample variance is increased; (3) the noise per pixel is decreased since more time can be spent integrating on this smaller patch of the sky.

For definiteness, suppose we hypothesize that there is a C component of the polarization with a power spectrum that has the ℓ dependence expected from inflation (as shown in Fig. 1 in Ref. [15]), but an unknown amplitude \mathcal{T} .⁴

We can predict the size of the error that we will obtain from the ensemble average of the curvature of the likelihood function (also known as the Fisher matrix) [26,27]. For example, consider the tensor signal. In such a likelihood analysis, the expected error will be $\sigma_{\mathcal{T}}$, where

$$\frac{1}{\sigma_{\mathcal{T}}^2} = \sum_{\ell} \left(\frac{\partial C_{\ell}^{\text{CC}}}{\partial \mathcal{T}} \right)^2 \frac{1}{(\sigma_{\ell}^{\text{CC}})^2}, \quad (1)$$

with similar equations for the other $C_{\ell}^{\text{XX}'}$.

Here, the $\sigma_{\ell}^{\text{XX}'}$ are the expected errors at individual ℓ for each of the XX' power spectra. These are given by (cf., Ref. [22])

$$\begin{aligned} \sigma_{\ell}^{\text{CC}} &= \sqrt{\frac{2}{f_{\text{sky}}(2\ell+1)}} \left(C_{\ell}^{\text{CC}} + f_{\text{sky}} w^{-1} B_{\ell}^{-2} \right), \\ \sigma_{\ell}^{\text{GG}} &= \sqrt{\frac{2}{f_{\text{sky}}(2\ell+1)}} \left(C_{\ell}^{\text{GG}} + f_{\text{sky}} w^{-1} B_{\ell}^{-2} \right), \\ \sigma_{\ell}^{\text{TG}} &= \sqrt{\frac{1}{f_{\text{sky}}(2\ell+1)}} \left[\left(C_{\ell}^{\text{TG}} \right)^2 + \left(C_{\ell}^{\text{TT}} + f_{\text{sky}} w^{-1} B_{\ell}^{-2} \right) \left(C_{\ell}^{\text{GG}} + f_{\text{sky}} w^{-1} B_{\ell}^{-2} \right) \right]^{1/2}, \end{aligned} \quad (2)$$

where $w = (t_{\text{pix}} N_{\text{pix}} T_0^2)/(4\pi s^2)$ is the weight (inverse variance) on the sky spread over 4π steradians, f_{sky} is the fraction of the sky observed, and t_{pix} is the time spent observing each of the N_{pix} pixels. The detector sensitivity is s and the average sky temperature is $T_0 = 2.73 \mu\text{K}$ (and hence all $C_{\ell}^{\text{XX}'}$ are measured in dimensionless $\Delta T/T$ units). The inverse weight for a full-sky observation is $w^{-1} = 2.14 \times 10^{-15} t_{\text{yr}}^{-1} (s/200 \mu\text{K} \sqrt{\text{sec}})^2$ with t_{yr} the total observing time in years. Finally, B_{ℓ} is the experimental beam, which for a Gaussian is $B_{\ell} = e^{-\ell^2 \sigma_{\theta}^2/2}$. We assume all detectors are polarized. As mentioned, all other $C_{\ell}^{\text{XX}'}$ cross terms are zero (in the usual cases, at least).

The CC and GG errors each have two terms, one proportional to C_{ℓ}^{XX} (the *sample variance*), and another proportional to w^{-1} (the *noise variance*). The TG error is more complicated since it involves the product of two different fields (T and G) on the sky.

There are several complications to note when considering these formulae: 1) We never have access to the actual $C_{\ell}^{\text{XX}'}$, but only to some estimate of the spectra; 2) the expressions

³This is not strictly true. In principle, as usual in Fourier analysis, less sky coverage merely limits the independent modes one can measure to have a spacing of $\delta\ell \gtrsim 180/\theta$. In practice, instrumental effects (detector drifts; “1/f” noise) will render the smallest of these bins unobservable.

⁴We define $\mathcal{T} \equiv 6C_2^{\text{TT,tens}}$ where $C_2^{\text{TT,tens}}$ is the tensor contribution to the temperature quadrupole moment expected for a scale-invariant spectrum.

only deal approximately with the effect of partial sky coverage; and 3) the actual likelihood function can be considerably non-Gaussian, so the expressions above do not really refer to “1 sigma confidence limits.”

Here, we are interested in the detectability of a polarization component; that is, what is the smallest polarization amplitude that we could confidently differentiate from zero? This answer in detail depends on the full shape of the likelihood function: the “number of sigma” that the likelihood maximum lies away from zero is related to the fraction of integrated likelihood between zero and the maximum. This gives an indication of how well the observation can be distinguished from zero power in the polarization. Toy problems and experience give us an approximate rule of thumb: the signal is detectable when it can be differentiated from the “null hypothesis” of $C_\ell^{\text{XX}} = 0$. Stated another (more Bayesian) way, for a fixed noise variance, as we increase the observed signal the fraction of probability below the peak increases rapidly when the sample variance—i.e., the estimated power—approaches the noise. Thus, on the one hand you need to observe enough sky to sufficiently decrease the sample variance, and a small enough noise that the sample variance dominates.

Thus, the ℓ component of the tensor signal (for example) is detectable if its amplitude is greater than

$$\sigma_\ell^{\text{CC}} = \sqrt{2/(2\ell + 1)} f_{\text{sky}}^{1/2} w^{-1} e^{\ell^2 \sigma_b^2}. \quad (3)$$

We then estimate the smallest tensor amplitude \mathcal{T} that can be distinguished from zero (at “1 sigma”) by using Eq. (1) with the null hypothesis $C_\ell^{\text{TT}} = 0$. Putting it all together, the smallest detectable tensor amplitude (scaled by the largest consistent with COBE) is

$$\frac{\sigma_{\mathcal{T}}}{\mathcal{T}} \simeq 1.47 \times 10^{-17} t_{\text{yr}} \left(\frac{s}{200 \mu\text{K}\sqrt{\text{sec}}} \right)^2 \left(\frac{\theta}{\text{deg}} \right) \Sigma_\theta^{-1/2}, \quad (4)$$

where

$$\Sigma_\theta = \sum_{\ell \geq (180/\theta)} (2\ell + 1) (C_\ell^{\text{CC}})^2 e^{-2\ell^2 \sigma_b^2}. \quad (5)$$

The expression for the GG signal from density perturbations is obtained by replacing C_ℓ^{CC} by C_ℓ^{GG} [and σ_ℓ^{GG} is the same as σ_ℓ^{CC} given in Eq. (3)].

For the TG cross-correlation, things are more complicated. First of all, the expression for σ_ℓ^{TG} in Eq. 2 has terms involving the temperature power spectra and observing characteristics. Second, we *know* that there is a temperature component on the sky, so we must pick a “null hypothesis” with the observed C_ℓ^{TT} . The TG moments also have covariances with the TT and GG moments (see Eqs. (3.28)–(3.30) in Ref. [22]), but these are zero for the null hypothesis of no polarization. Hence, with the null hypothesis of no polarization, the variance with which each C_ℓ^{TG} can be measured is

$$\sigma_\ell^{\text{TG}} = \sqrt{1/f_{\text{sky}}(2\ell + 1)} \left[f_{\text{sky}} w^{-1} e^{\ell^2 \sigma_b^2} (C_\ell^{\text{TT}} + f_{\text{sky}} w^{-1} e^{\ell^2 \sigma_b^2}) \right]^{1/2}. \quad (6)$$

Thus, the dependence on s is more complicated than in Eq. (6), so the end result for the polarization sensitivity achievable by cross-correlating with the temperature does not scale simply with s or t_{yr} as it does for GG and CC.

IV. DETECTABILITY OF DENSITY-PERTURBATION SIGNAL

Since the polarization has yet to be detected, the obvious first goal of a current experiment should be to detect unambiguously the polarization. In the standard theory with adiabatic perturbations somehow laid down prior to last scattering, the G polarization is inevitable. Density perturbations will thus produce a nonzero GG power spectrum and a TG power spectrum. We discuss the detectability of polarization from only the GG signal or the TG signal individually, and then from the combination of both signals.

A. The GG signal

We have calculated the detectability of the polarization from density perturbations (using only the GG power spectrum), and results are shown in Fig. 1. Here, we ask the following: Suppose there is a polarization signal with an ℓ dependence characteristic of density perturbations but of unknown amplitude. What is the smallest polarization amplitude that could be distinguished from the null hypothesis of no polarization? The short-dashed curves (which coincide with the solid curves for small survey widths) in Fig. 1 show the smallest polarization amplitude \mathcal{S} (scaled by that expected for a COBE-normalized CDM model) detectable (at 3σ) by an experiment with detector sensitivity s that maps the polarization only on a square region of the sky with a given width. The curves are (from top to bottom) for fwhm beamwidths of 1, 0.5, 0.3, 0.2, 0.1, 0.05, and 0.01 degrees. The results scale with the square of the detector sensitivity and inversely to the duration of the experiment. Any experiment that has a (σ_S/\mathcal{S}) smaller than unity should be able to detect the polarization expected in a CDM model at $> 3\sigma$. Fig. 1 shows that an experiment with comparable s can in a few months achieve the same signal-to-noise with the GG power spectrum as MAP.

B. The TG signal

We have also done the same analysis for the temperature/polarization cross correlation (the TG power spectrum), and the results are indicated by the long-dashed curves in Fig. 1. Here we ask, what is the smallest polarization signal that could be distinguished from the null hypothesis of no polarization by looking for the expected temperature-polarization cross-correlation? First of all, the analog of Eq. (3) for GG is given for TG by Eq. (6). Thus, cosmic variance in the temperature map comes into play even if we investigate the null hypothesis of no polarization. As a result, the detectability of the polarization from temperature-polarization cross-correlation does not scale simply with the instrumental sensitivity s (and this is why we present results for detectability in four panels for four different values of s in Fig. 1 rather than on one panel as we will for the curl component in Fig. 2). However, comparing the long-dash curves in all four panels, we see that for $s \lesssim 200 \mu\text{K}\sqrt{\text{sec}}$ (reasonable values for just about any future experiments), the detector-noise term in Eq. (6) is less important than the C_ℓ^{TT} term, so the result for σ_S/\mathcal{S} scales with s .

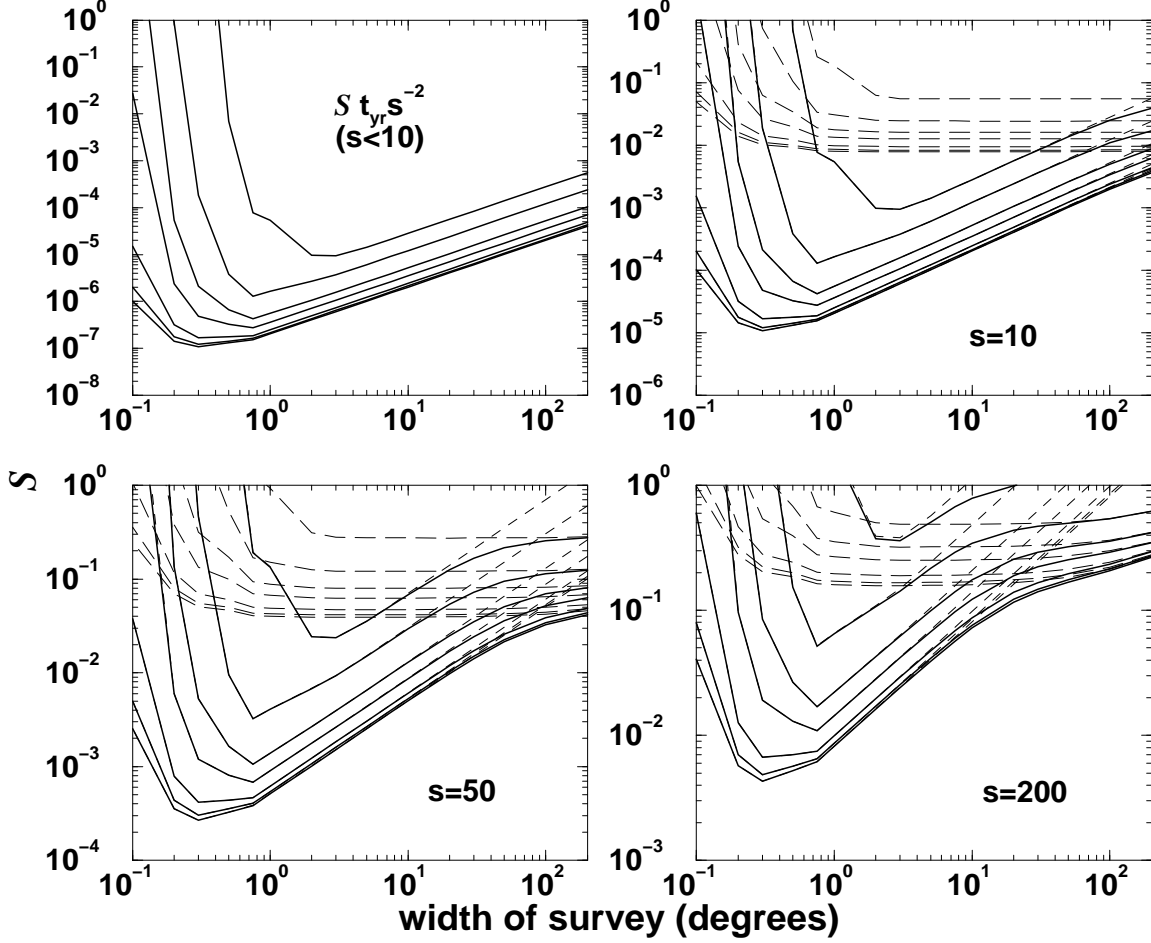


FIG. 1. The smallest amplitude \mathcal{S} of the polarization signal from density perturbations (scaled by that expected from a COBE-normalized CDM model) that could be detected at 3σ with various values of the detector sensitivity s (given in units of $\mu\text{K}\sqrt{\text{sec}}$) for an experiment that runs for one year and maps a square region of the sky of a given width. The long-dash curves show the sensitivities achievable by cross-correlating with the CMB temperature. The short-dash curves show sensitivities achievable using only the polarization autocorrelation function (the GG power spectrum). The solid curves show results achievable using both the GG and TG power spectra. The curves are (from top to bottom) for fwhm beamwidths of 1, 0.5, 0.3, 0.2, 0.1, 0.05, and 0.01 degrees. For $s < 10 \mu\text{K}\sqrt{\text{sec}}$, the sensitivity comes entirely from the polarization auto-correlation and scales as s^2 and inversely with t_{yr} , as shown in the top left-hand panel.

C. Combining the TG and GG Signal

Comparing the long- and short-dash curves in Fig. 1, we see that the polarization sensitivity obtained by looking for a temperature-polarization cross-correlation improves on that obtained from the polarization auto-correlation (for fixed angular resolution and detector sensitivity) only for nearly full-sky surveys with $s \gtrsim 50 \mu\text{K}\sqrt{\text{sec}}$. Thus, the sensitivity of MAP (full-sky and $s \simeq 150 \mu\text{K}\sqrt{\text{sec}}$) to polarization will come primarily from cross-correlating with the temperature map, while the signal-to-noise for polarization auto-correlation and temperature-polarization cross-correlation should be roughly comparable for Planck. The Figure also indicates that in an experiment with $s \lesssim 100 \mu\text{K}\sqrt{\text{sec}}$ that maps only a small fraction of the sky (widths $\lesssim 10^\circ$), the polarization is more easily detected via polarization auto-correlations; cross-correlating with the temperature should not significantly improve the prospects for detecting the polarization in such experiments.

The total sensitivity achievable using both TG and GG together is obtained by adding the sensitivities from each in quadrature.⁵ The solid curves in Fig. 1 show the polarization sensitivities achievable by combining the GG and TG data. For $s \lesssim 10 \mu\text{K}\sqrt{\text{sec}}$, the sensitivity comes entirely from the polarization auto-correlation and scales as s^2 , as shown in the top left-hand panel.

We see that the sensitivity to the polarization can improve as the angular resolution is improved all the way down to 0.01 degrees, and the ideal survey size varies from 2–3 degrees (for an angular resolution of 1 degree) to a fraction of a degree for better angular resolution.

V. DETECTABILITY OF THE CURL COMPONENT

Consider next the C component, which can tell us about the amplitude of gravitational waves produced, for example, by inflation. We have carried out the exercise as for the scalar signal. As above we hypothesize that there is a C component of the polarization with an unknown amplitude \mathcal{T}

Results are shown in Fig. 2. Plotted there is the smallest gravitational-wave (i.e., tensor) amplitude \mathcal{T} detectable at 3σ by an experiment with a detector sensitivity $s = 10 \mu\text{K}\sqrt{\text{sec}}$ that maps a square region of the sky over a year with a given beamwidth. The horizontal line shows the upper limit to the tensor amplitude from COBE. The curves are (from top to bottom) for fwhm beamwidths of 1, 0.5, 0.3, 0.2, 0.1, and 0.05 degrees. The results scale with the square of the detector sensitivity and inversely to the duration of the experiment.

The sensitivity to the tensor signal is a little better with an 0.5-degree beam than with a 1-degree beam, but even smaller angular resolution does not improve the sensitivity much. And with a resolution of 0.5 degrees or better, the best survey size for detecting this tensor signal is about 3 to 5 degrees. If such a fraction of the sky is surveyed, the sensitivity to a tensor signal (rms) will be about 30 times better than with a full-sky survey with the same detector sensitivity and duration (and thus 30 times better than indicated in Refs. [14,15].

⁵In principle, there are cross terms between TG and GG in the correlation matrix. However, for the null hypothesis of no polarization, these are zero; cf., Eq. (3.29) in Ref. [22].

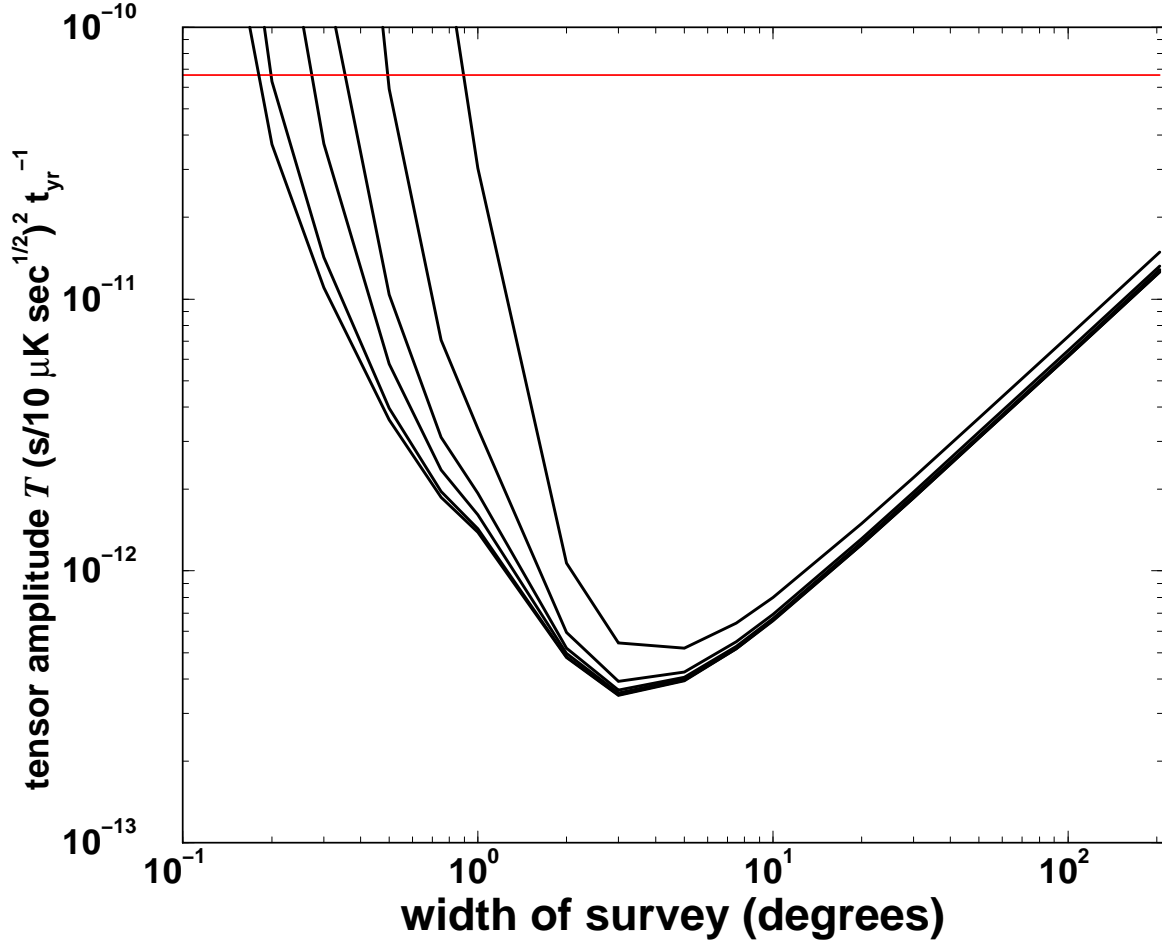


FIG. 2. The smallest tensor amplitude \mathcal{T} that could be detected at 3σ with an experiment with a detector sensitivity $s = 10 \mu\text{K}\sqrt{\text{sec}}$ that runs for one year and maps a square region of the sky of a given width. The result scales with the square of the detector sensitivity and inversely with the duration of the experiment. The curves are (from top to bottom) for fwhm beamwidths of 1, 0.5, 0.3, 0.2, 0.1, and 0.05 degrees. The horizontal line shows the upper limit to the tensor amplitude from COBE.

Thus, a balloon experiment with the same detector sensitivity as MAP could in principle detect the same tensor amplitude in a few weeks that MAP would in a year. (A width of 200 degrees corresponds to full-sky coverage.)

The tensor amplitude is related to the energy scale of inflation⁶ by $\mathcal{T} = (E_{\text{infl}}/7 \times 10^{18} \text{ GeV})^4$, and COBE currently constrains $E_{\text{infl}} \lesssim 2 \times 10^{16} \text{ GeV}$ [14,28]. Thus with Fig. 2, one can determine the inflationary energy scale accessible with any given experiment.

VI. SOME DETAILS AND INSIGHT

Fig. 3 is intended to provide some additional insight into the results shown in Figs. 1 and 2. Fig. 3 plots the summands (with arbitrary normalization) from Eq. (5) for Σ_θ for the CC and GG signals for a full-sky map with perfect angular resolution. It also shows the analogous summand for TG. The detectability of each signal (CC, GG, and TG) is inversely proportional to the square root of the area under each curve. A finite beamwidth (and/or instrumental noise) would reduce the contribution from higher ℓ 's and a survey area less than full-sky would reduce the contribution from lower ℓ 's. The Figure illustrates that the CC signal is best detected with $\ell \lesssim 200$ and the GG signal is best detected with $\ell \simeq 200 - 1200$, as may have been surmised from Figs. 1 and 2. The TG signal is spread over a larger range of ℓ 's. In particular, note that very little of Σ_θ comes from $\ell \lesssim 10$ in any case, so the loss of the $\ell \lesssim 10$ modes that comes with survey regions smaller than $10 \times 10 \text{ deg}^2$ does not significantly affect the detectability of the polarization signals.

And now for some historical perspective. Although not shown, the Σ_θ for the temperature power spectrum TT peaks *very* sharply at low ℓ (it essentially falls off as ℓ^{-3} for a nearly scale-invariant spectrum [$\ell(\ell+1)C_\ell \simeq \text{const}$] such as that observed). Thus, in retrospect, the COBE full-sky scan was indeed the best strategy for detecting the temperature anisotropy. An equal-time survey of a smaller region of the sky would have made detection far less likely.

VII. MODEL INDEPENDENCE OF THE RESULTS

In Section IV we used a standard-CDM model for our calculations, and it is natural to inquire whether and/or how our results depend on this assumption. The purpose of this Section is to illustrate that the results shown above are, to a large extent, *independent* of the gross features and details of the structure-formation model as long as we (1) use the BBN baryon density and (2) demand that the model reproduce the degree-scale anisotropy observed by several recent experiments.

To make this case, we have considered a number of models in which the CMB power spectrum passes through recent data points near $\ell \sim 200$, as shown in Fig. 4. The models are listed in Table I. The C_ℓ^{GG} polarization power spectrum for each model is shown in Fig. 5. The detectability of the polarization—*à la* Fig. 1—in each of these models is shown

⁶The energy scale of inflation is defined here to be the fourth root of the inflaton-potential height.

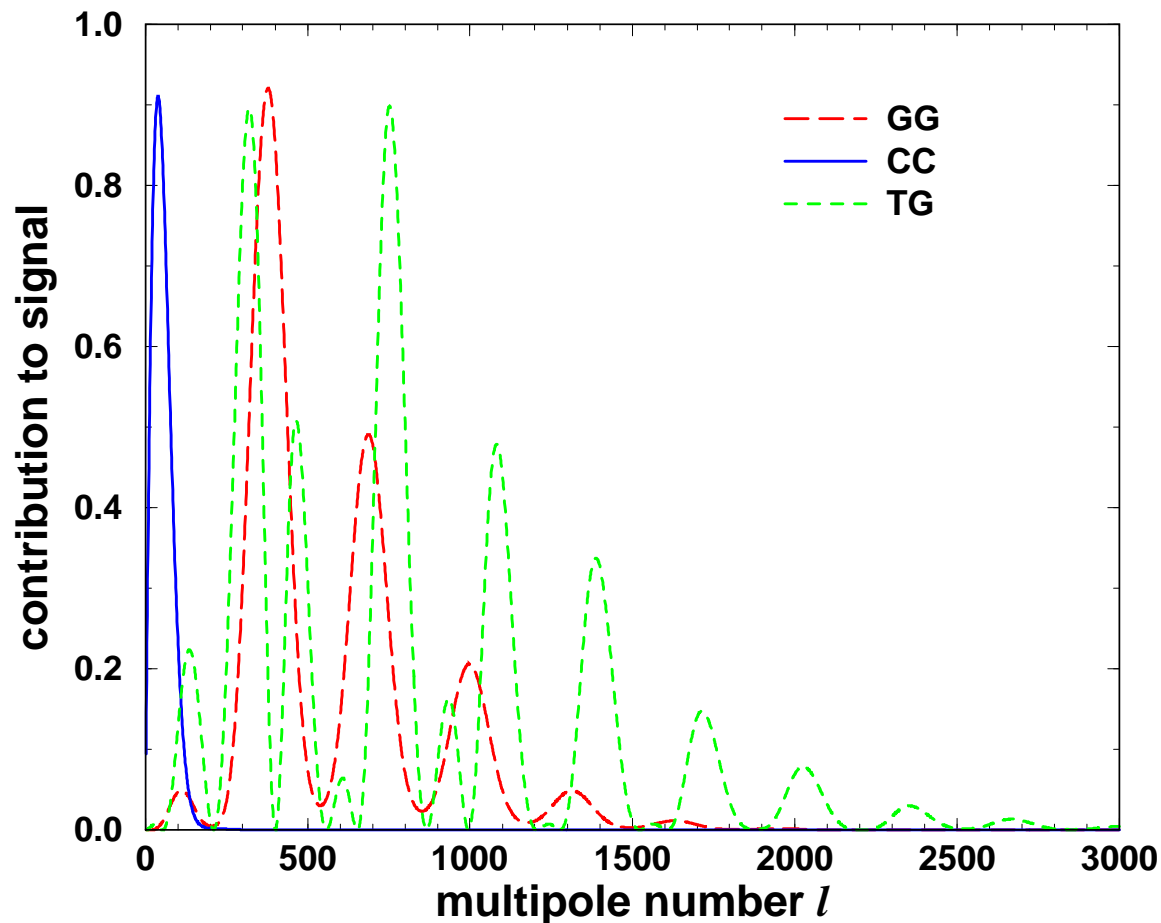


FIG. 3. The summands for Σ_θ for the CC, TG, and GG signals for a full-sky map with perfect angular resolution and no detector noise. The signal-to-noise of each signal is proportional to the inverse of the square root of the area under the curve. A beam of finite width θ_{fwhm} would reduce the contribution from $\ell > 200(\theta_{\text{fwhm}}/\text{deg})^{-1}$'s and a survey of width θ would reduce the contribution from $\ell < (\theta/180 \text{ deg})$'s.

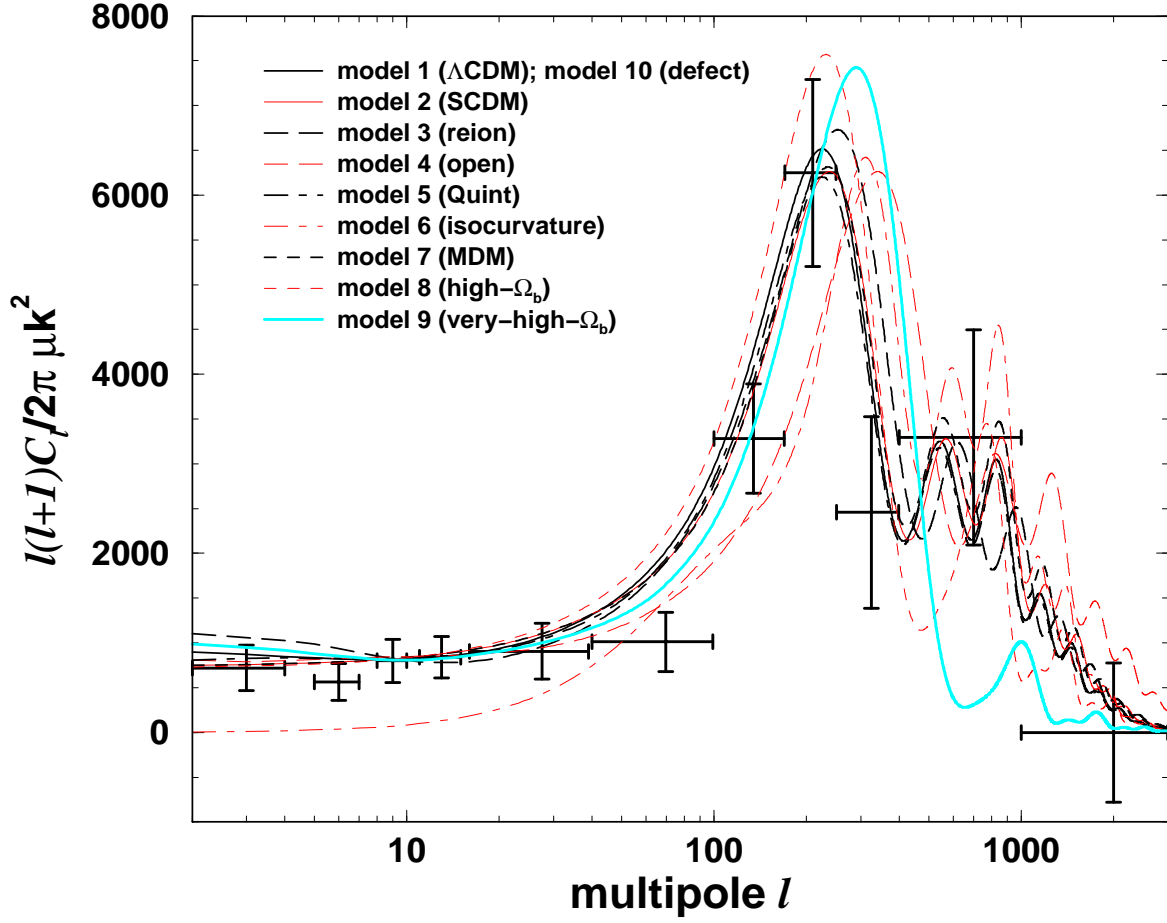


FIG. 4. The temperature power spectra for the structure-formation models listed in Table I. The models were all chosen to fit (by eye) the data points (see Ref. [25] for how the data points were compiled) near $\ell \sim 200$.

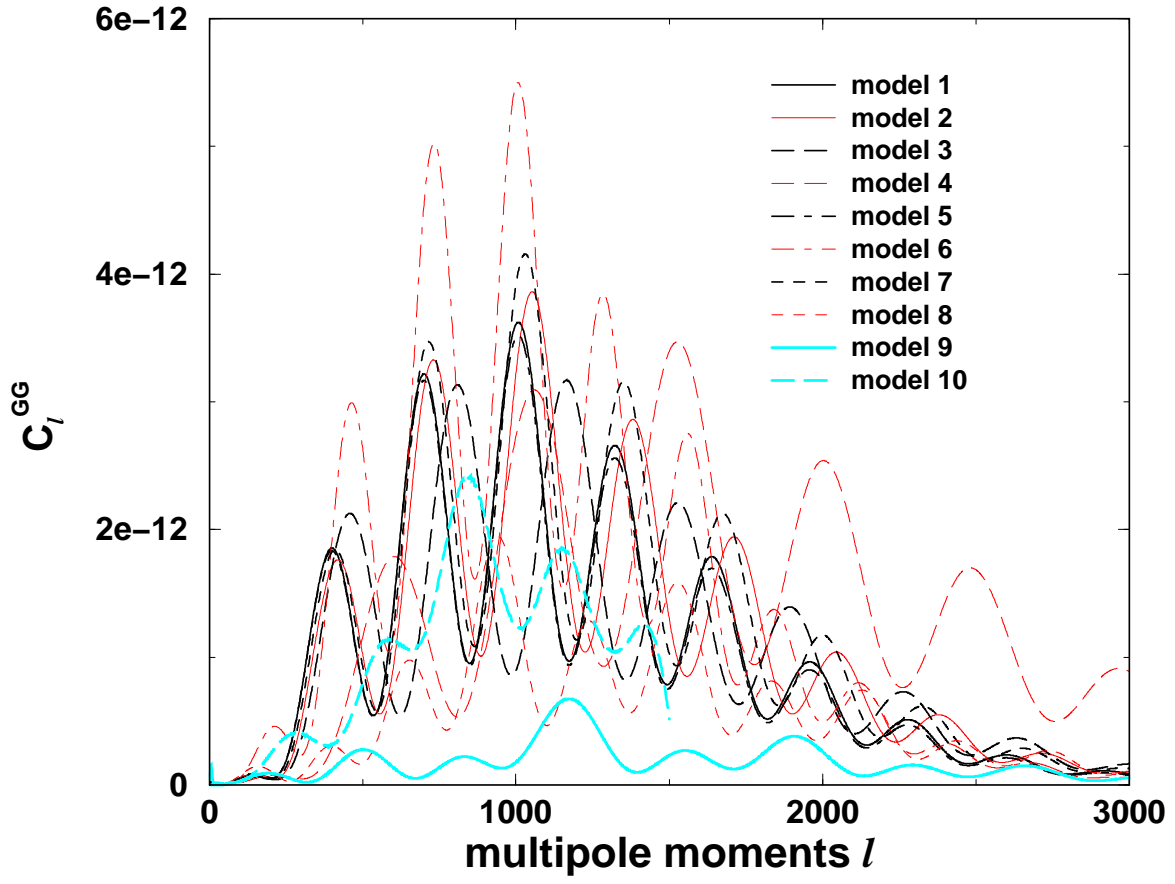


FIG. 5. The GG polarization power spectra for each of the models listed in Table I.

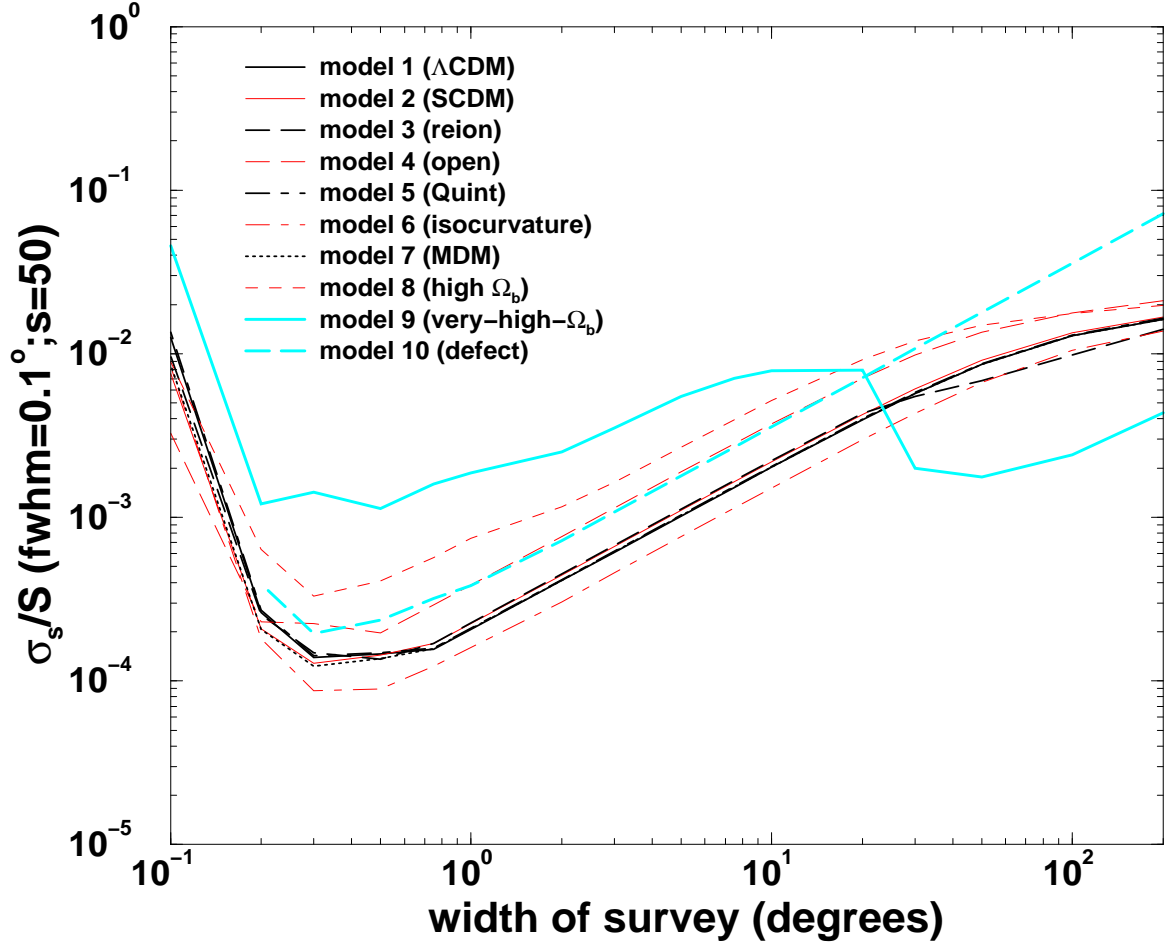


FIG. 6. The detectability of the polarization (as plotted in Fig. 1) for each of the models listed in Table I.

	model	Ω_0	Ω_Λ	Ω_ν	h	n	$\Omega_b h^2$	τ_r
1	Λ CDM	1	0.7	0	0.65	1.0	0.020	0
2	SCDM	1	0	0	0.40	1.0	0.019	0
3	reion	1	0.7	0	0.50	1.0	0.019	0.2
4	open	0.5	0	0	0.50	1.0	0.020	0
5	Quint	1	0.52	0	0.51	1.0	0.019	0
6	isocurvature	1	0	0	0.65	3.0	0.021	0
7	MDM	1	0	0.5	0.40	1.0	0.019	0
8	high- Ω_b	1	0	0	0.70	1.0	0.058	0
9	very-high- Ω_b	1	0	0	0.60	0.95	0.144	0.5
10	defect	1	0	0	0.65	N/A	0.019	0

TABLE I. Parameters for the models in Figs. 4, 5, and 6. In model 5, the cosmological constant is actually a quintessence component with an equation of state $w = -0.5$. We get the power spectra for model 10 (the defect model) by scaling the power spectra of Ref. [29] so that the C_ℓ^{TT} fit the data near the first peak. Since Ref. [29] uses $\Omega_b h^2 = 0.0125$, we use the scaling discussed in the text [3,30] to approximate the polarization power spectrum for $\Omega_b h^2 = 0.02$.

in Fig. 6. All of the models (except the high-baryon-density models) have the BBN baryon-to-photon ratio, $\Omega_b h^2 = 0.02$. Fig. 5 shows that all models with the BBN baryon density produce roughly the same amount of polarization, and Fig. 6 shows more precisely that the detectabilities are all similar. The only models in which the polarization signal is significantly smaller (and accordingly harder to detect) are those with a baryon-to-photon ratio that considerably exceeds the BBN value.

So why is this? Heuristically, we expect the polarization amplitude to be proportional to the temperature-anisotropy amplitude, and we have fixed this. This explanation is close, but still only partially correct. More accurately, the polarization comes from peculiar velocities (the “dipole” [30]) at the surface of last scatter [3]. The peculiar-velocity amplitude is indeed proportional to the density-perturbation amplitude that produces the peak in the temperature power spectrum, but the constant of proportionality depends on the baryon density [3,30]; the peculiar velocity (and thus the polarization) is larger for smaller $\Omega_b h^2$ (and the dependence is actually considerably weaker than linear). We also know that the troughs in the temperature power spectrum are filled in by the peculiar velocities. Therefore, the polarization amplitude should actually be proportional to the amplitude of the (yet-undetermined) trough in the power spectrum, rather than the peak that has been measured. Having fixed the peak height, the amplitude of the trough—and thus the peculiar velocity—in turn depends only on the baryon density, $\Omega_b h^2$.

In this way, the polarization amplitude depends primarily on the baryon-to-photon ratio, itself proportional to $\Omega_b h^2$. These arguments further suggest that if the baryon density is significantly higher than that allowed by BBN, then the polarization amplitude will be smaller, and accordingly harder to detect. There are many good reasons to believe that the BBN prediction for the baryon density is robust. However, it has also been pointed out

that some problems (e.g., the baryon fraction in clusters and a reported excess in power on $100 h^{-1}$ Mpc scales) can be solved if we disregard the BBN constraint and consider a much larger baryon density (see e.g., Ref. [31]). To illustrate, we also include in Figs. 4, 5, and 6 results from a high-baryon-density (i.e., $\Omega_b h^2 = 0.144$) model [31], and as expected, the polarization amplitude is decreased relative to the temperature-fluctuation amplitude. We conclude that as long as the baryon density is not much larger than that allowed by BBN, the results shown in Fig. 1 should be model-independent, but that the polarization may be significantly smaller if the baryon-to-photon ratio is significantly higher.

VIII. CONCLUSIONS

We have carried out calculations that will help assess the prospects for detection of polarization with various experiments. Our results can be used to forecast the signal-to-noise for the polarization signals expected from density perturbations and from gravitational waves in an experiment of given sky coverage, angular resolution, and instrumental noise. Even after the polarization has been detected, our results will provide a useful set (although not unique) of figures of merit for subsequent polarization experiments. Of course, the “theoretical” factors considered here must be weighed in tandem with those that involve foreground subtraction and experimental logistics in the design or evaluation of any particular experiment. (As with temperature-anisotropy experiments, these usually encourage increasing the signal-to-noise to better distinguish systematic effects.)

In contrast to temperature anisotropies which show power on all scales [i.e., $\ell(\ell+1)C_\ell \sim \text{const}$], the polarization power peaks strongly at higher ℓ . Hence the signal-to-noise in a polarization experiment of fixed flight time and instrumental sensitivity may be improved by surveying a smaller region of sky, unlike the case for temperature-anisotropy experiments. The ideal survey for detecting the curl component from gravitational waves is of order 2–5 degrees, and the sensitivity is not improved much for angular resolutions smaller than 0.2 degrees.⁷ The polarization signal from density perturbations is peaked at still smaller angular scales, and may be better accessed by mapping an even smaller region of sky (again, keeping in mind the caveats mentioned above).

Our numerical experiments and some physical arguments indicate that the measured degree-scale temperature anisotropy fixes the polarization amplitude in a model-independent way as long as we use a fixed baryon density. Thus, if the baryon density is known from BBN, then *any experiment for which the curves in Fig. 1 fall below unity is guaranteed a 3σ detection of the CMB polarization*. A non-detection would indicate unambiguously a baryon density significantly higher than that predicted by BBN.

⁷Of course, better angular resolution and a larger survey area may be required to distinguish the gravitational-wave signal from a possible curl component from some foregrounds, nonlinear late-time effects [32,33], and/or instrumental artifacts.

ACKNOWLEDGMENTS

We thank L. Knox for providing the updated CMB data, and S. Hanany, A.T. Lee and the whole MAXIMA team for inspiring some of the work described herein. This work was supported at Columbia by a DoE Outstanding Junior Investigator Award, DEFG02-92-ER 40699, NASA NAG5-3091, and the Alfred P. Sloan Foundation, and at Berkeley by NAG5-6552 and NSF KDI grant 9872979.

REFERENCES

- [1] M. J. Rees, *Astrophys. J. Lett.* **153**, L1 (1968).
- [2] A. Kosowsky, *Ann. Phys.* **246**, 49 (1996).
- [3] M. Zaldarriaga and D. D. Harari, *Phys. Rev. D* **52**, 3276 (1995).
- [4] M. Zaldarriaga, *Phys. Rev. D* **55**, 1822 (1997).
- [5] A. Kosowsky, *astro-ph/9811163*.
- [6] M. Zaldarriaga and D. N. Spergel, *Phys. Rev. Lett.* **79**, 2180 (1997).
- [7] M. Kamionkowski, A. Kosowsky, and A. Stebbins, *Phys. Rev. Lett.* **78**, 2058 (1997).
- [8] U. Seljak and M. Zaldarriaga, *Phys. Rev. Lett.* **78**, 2054 (1997).
- [9] A. Kosowsky and A. Loeb, *Astrophys. J.* **469**, 1 (1996).
- [10] D. D. Harari, J. Hayward, and M. Zaldarriaga, *Phys. Rev. D* **55**, 1841 (1996).
- [11] E. S. Scannapieco and P. G. Ferreira, *Phys. Rev. D* **56**, 4578 (1997).
- [12] A. Lue, L. Wang, and M. Kamionkowski, *Phys. Rev. Lett.* **83**, 1503 (1999).
- [13] N. Lepora, *gr-qc/9812077*.
- [14] M. Kamionkowski and A. Kosowsky, *astro-ph/9904108*, *Ann. Rev. Nucl. Part. Sci.*, in press (1999).
- [15] M. Kamionkowski and A. Kosowsky, *Phys. Rev. D* **57**, 685 (1998).
- [16] J. Lesgourgues et al., *gr-qc/9906098*.
- [17] W. H. Kinney, *Phys. Rev. D* **58**, 123506 (1998).
- [18] M. Zaldarriaga, U. Seljak, and D. N. Spergel, *Astrophys. J.* **488**, 1 (1997).
- [19] E. J. Copeland, I. J. Grivell, and A. R. Liddle, *Mon. Not. R. Astron. Soc.* **298**, 1233 (1998).
- [20] J. Magueijo and M. P. Hobson, *Phys. Rev. D* **56**, 1908 (1997).
- [21] M. P. Hobson and J. Magueijo, *Mon. Not. R. Astron. Soc.* **283**, 1133 (1996).
- [22] M. Kamionkowski, A. Kosowsky, and A. Stebbins, *Phys. Rev. D* **55**, 7368 (1997).
- [23] M. Zaldarriaga and U. Seljak, *Phys. Rev. D* **55**, 1830 (1997).
- [24] J. R. Bond, A. H. Jaffe, and L. Knox, *Phys. Rev. D* **57**, 2117, (1998).
- [25] J. R. Bond, A. H. Jaffe, and L. Knox, *Phys. Rev. D*, submitted (1999), *astro-ph/9808264*.
- [26] G. Jungman, M. Kamionkowski, A. Kosowsky, and D. N. Spergel, *Phys. Rev. Lett.* **76**, 1007 (1996).
- [27] G. Jungman, M. Kamionkowski, A. Kosowsky, and D. N. Spergel, *Phys. Rev. D* **54**, 1332 (1996).
- [28] J. P. Zibin, D. Scott, and M. White, *astro-ph/9901028*.
- [29] U. Seljak, U.-L. Pen, and N. Turok, *Phys. Rev. Lett.* **79**, 1615 (1997).
- [30] W. Hu and N. Sugiyama, *Astrophys. J.* **444**, 489 (1995).
- [31] D. Eisenstein et al., *Astrophys. J. Lett.* **494**, L1 (1998).
- [32] M. Zaldarriaga and U. Seljak, *Phys. Rev. D* **58**, 023003 (1998).
- [33] W. Hu, *astro-ph/9907103*.